https://doi.org/10.48048/tis.2022.5689

Calculation of the Halfwidth and the Activation Energy for the Soft Raman Modes in the Brominated Compounds of Tris-Sarcosine Calcium Chloride

Ali Kiraci

Inter-Curricular Courses Department, Cankaya University, Ankara, Turkey

(Corresponding author's e-mail: akiraci@cankaya.edu.tr)

Received: 6 July 2021, Revised: 6 September 2021, Accepted: 13 September 2021

Abstract

This letter contributes how to calculate the anomalous behavior for the damping constant (halfwidth) of the ferroelectric Tris-Sarcosine Calcium Chloride (TSSC) and its brominated compounds $TSSC_{1-x}Br_x$ (x = 0.13, 0.42 and 0.60) from the wavenumber data of the soft modes below the phase transition temperature of T_C. The pseudospin-phonon coupled (PS) and the energy fluctuation (EF) models derived from the dynamical Ising model were used. Both PS and EF models have been used to contribute understanding the temperature dependence of the phase transition mechanism of $TSSC_{1-x}Br_x$. In addition, values of the activation energy for $TSSC_{1-x}Br_x$ (x = 0, 0.13, 0.42 and 0.60) were extracted from the damping constant as calculated from both models (PS and EF). Our results indicate order-disorder type phase transition for $TSSC_{1-x}Br_x$.

Keywords: Halfwidth (damping constant), Soft mode, Ising model, Activation energy, $TSSC_{1-x}Br_x$

Introduction

As a member of uniaxial ferroelectric Tris-Sarcosine Calcium Chloride (TSSC), $(CH_3NHCH_2COOH)_3NaCl$, undergoes a phase transition of a second order type from paraelectric to ferroelectric at around 130 K depending on the sample preparation [1-3]. This crystal has unusual (perhaps unique) orthorhombic symmetry in both high (paraelectric) and low (ferroelectric) phases with 4 formula units per unit cell characterized by a space groups D_{2h}^{16} (Pnma) and C_{2v}^{9} ($Pna2_1$), respectively [4,5]. Since there is no well-defined limit for the structural phase transition mechanism, whether order-disorder or displacive type, a number of contoversial conclusions have been reported for this crystal. The small Curie constant (C = 58 K) and large entropy of transition (ΔS = 0.38 cal/mol.K) [6] and the small spontaneous polarization (0.27 $\mu C/cm^2$) [6] were considered as a sign for the order-disorder type transition. On the other hand, the existence of the soft mode in the ferroelectric phase [7,8] was considered as a sign for the displacive type transition. Various experimental methods including Raman spectroscopy [8-10], Infrared spectroscopy [11], x-ray diffraction [12], EPR [13], backward-wave oscillator method [14], NMR [15-17], and elasticity [18] have been reported in the literature. In addition, some theoretical works have been carried out. Namely, the pseudospin-phonon coupling theory [19] has been used to explain the Raman and infrared spectra. A cluster model [20] on the other hand has been used to interpret the pressure-temperature phase diagram of TSSC. It is stated that as the hydrostatic pressure increases the transition temperature Tc increases also [21]. Although the isomorphous Tris-Sarcosine Calcium Bromide (TSSB) does not show ferroelectricity down to liquid helium temperature [22], in the mixed crystal systems of the chloride and bromide, $TSSC_{1-x}Br_x$, ferroelectricity exists for $x \leq 0.75$ [23]. It is also reported that [24] the transition temperature T_C in $TSSC_{1-x}Br_x$ decreases as x increases.

TSSC is suitable for device applications that require an enhanced electrical or strain response function since the phase transition in it can easily be tuned by chemical doping of bromine and iodine. One such application involves cryogenic solid-state refrigeration employing the electro-caloric effect as the temperature lowered toward the 0 K [25].

The damping constant (halfwidth), in general, can be calculated from measured dielectric constant data [26] or from the measured intensity data [27] within the framework of the classical pseudo-harmonic models. Both models (PS and EF) represent a phenomenological fit to the experimental data of the

relaxation rate for ferroelectric materials based on the order parameter (spontaneous polarization or wavenumber).

In this study, the temperature dependence of the halfwidth (damping constant) for the soft Raman modes in $TSSC_{1-x}Br_x$ (x = 0, 0.13, 0.42 and 0.60) was calculated below the phase transition temperature T_C using the pseudospin-phonon coupled (PS) model [28,29] and the energy fluctuation (EF) model [30]. For this calculation, we use the temperature dependence of the observed [9] wavenumber of the soft Raman modes as an order parameter. The halfwidths calculated from both models (PS and EF) were fitted to the observed [9] data and the fitted parameters were determined. In addition, values of the activation energy for the compounds studied here were extracted by using the halfwidth calculated from both PS and EF models in the ferroelectric phases. We used these 2 models (PS and EF) in our previous studies to calculate some thermodynamic quantities such as the damping constant, the frequency, the relaxation time and the activation energy for $BaTiO_3$ [31,32], KH_2PO_4 [33], $Cd_2Nb_2O_7$ [34], $PbTiO_3$ [35], $SrZrO_3$ [36], PZT [37] and very recently for $LiTaO_3$ [38] and $SrTiO_3$ [39].

Below, "Calculations and results" was given in section 2. In section 3, the results were discussed and the "Conclusions" part was given in section 4.

Calculations and results

Laulicht and Luknar [28] derived an expression (pseudospin-phonon coupled model, PS) to calculate the temperature dependence of the halfwidth near the transition temperature T_C using the calculations of Lahajnar *et al*. [40] on the basis of the damping constant (halfwidth) expression of Matsushita [41] which reads as;

$$\Gamma_{SP}(k_\upsilon, \omega_\upsilon) = \Gamma_0' + A'(1 - P^2) \ln \left[\frac{T_C}{T - T_C(1-P^2)}\right] \quad (1)$$

The damping constant $\Gamma_{SP}(k_\upsilon, \omega_\upsilon)$ appearing in Eq. (1) is attributed to the pseudospin-phonon interaction of the υ-th phonon with the wave vector k where ω_υ is the peak frequency, Γ_0' is the background damping constant, A' is a weakly temperature dependent constant and P is the spontaneous polarization (order parameter). On the other hand, Schaack and Winterfeldt [27] derived another expression to calculate the temperature dependence of the damping constant (halfwidth) by considering the pseudospin-phonon coupling which causes a shift in the phonon frequencies (Energy fluctuation model, EF) given by;

$$\Gamma_{SP} = \Gamma_0 + A[\frac{T(1-P^2)}{T - T_C(1-P^2)}]^{1/2} \quad (2)$$

where Γ_0 is the background damping constant and A is a constant as before. Regarding Eq. (2), it is reported that [28,29] the shift in the phonon frequency is proportional to the polarization $P(k = 0)$ which causes a critical broadening due to the energy fluctuation of this mode.

The spontaneous polarization (order parameter) P appearing in both PS and EF models Eqs. (1) - (2) can take any value between 0 and 1 and it can be calculated within the framework of the molecular field theory as stated before [41] which reads as;

$$P \approx \begin{cases} 1 - 2\exp\left(\frac{-2T_C}{T}\right) & T \langle\langle T_C \\ \left\{3\left(1 - \frac{T}{T_C}\right)\right\}^{\frac{1}{2}} & 0 \langle (T_C - T) \langle T_C \\ 0 & T_C \langle T \end{cases} \quad (3)$$

Table 1 Maximum values of the observed [9] wavenumbers (ω_{max}) and transition temperatures T_C for $TSSC_{1-x}Br_x$ (x = 0, 0.13, 0.42 and 0.60).

Crystal	ω_{max} (cm^{-1})	T_C (K)
$TSSC_{1-x}Br_x$ (x = 0)	31.6	132
$TSSC_{1-x}Br_x$ (x = 0.13)	29.8	121
$TSSC_{1-x}Br_x$ (x = 0.42)	24.8	88
$TSSC_{1-x}Br_x$ (x = 0.60)	19.5	61

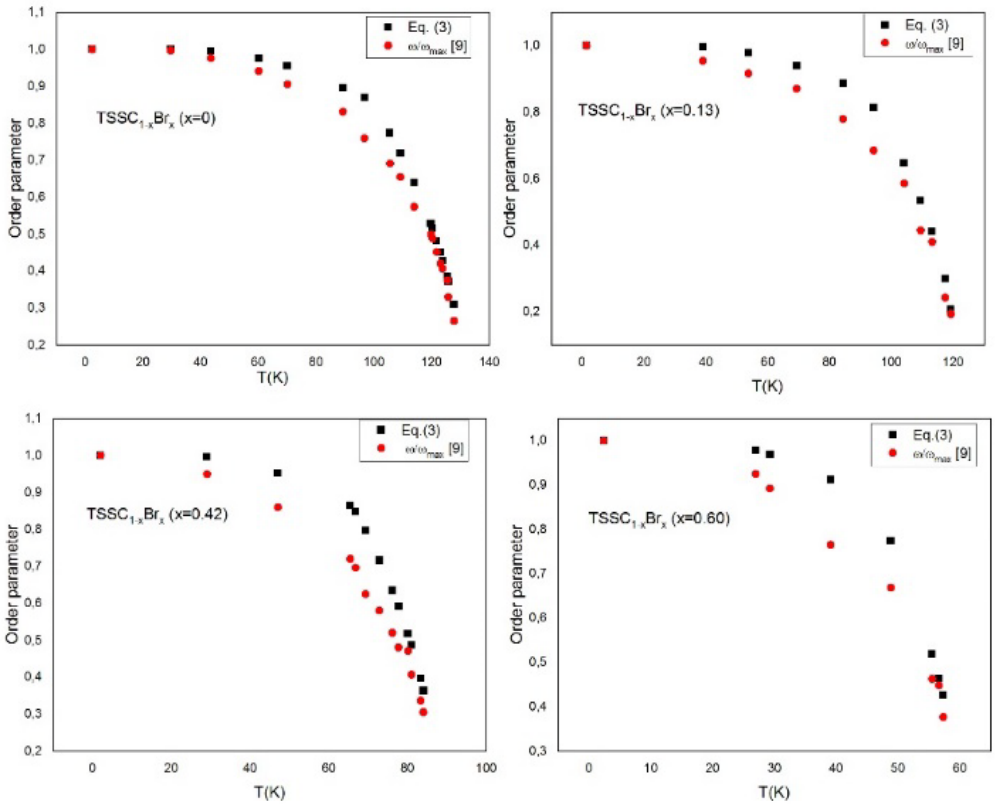

Figure 1 The temperature dependence of the order parameter P Eq. (3) and the experimental [9] normalized wavenumber ω/ω_{max} of the soft Raman modes in the ferroelectric phases of $TSSC_{1-x}Br_x$ (x = 0, 0.13, 0.42 and 0.60).

Table 2 Values of the fitted parameters for the damping constant Γ_{SP} in Eqs. (1) - (2) using the observed data [9] in the ferroelectric phases of $TSSC_{1-x}Br_x$ (x = 0, 0.13, 0.42 and 0.60).

Crystal	Γ_0'(cm^{-1})	A'(cm^{-1})	Γ_O(cm^{-1})	A(cm^{-1})	Temperature interval (K)
$TSSC_{1-x}Br_x$ (x = 0)	2.02	4.95	1.57	3.39	2.4 < T < 127.8
$TSSC_{1-x}Br_x$ (x = 0.13)	2.21	2.78	2.17	1.67	1.5 < T < 119.3
$TSSC_{1-x}Br_x$ (x = 0.42)	2.53	2.79	2.23	1.96	2.1 < T < 84.2
$TSSC_{1-x}Br_x$ (x = 0.60)	2.76	2.38	2.44	1.74	2.4 < T < 57.3

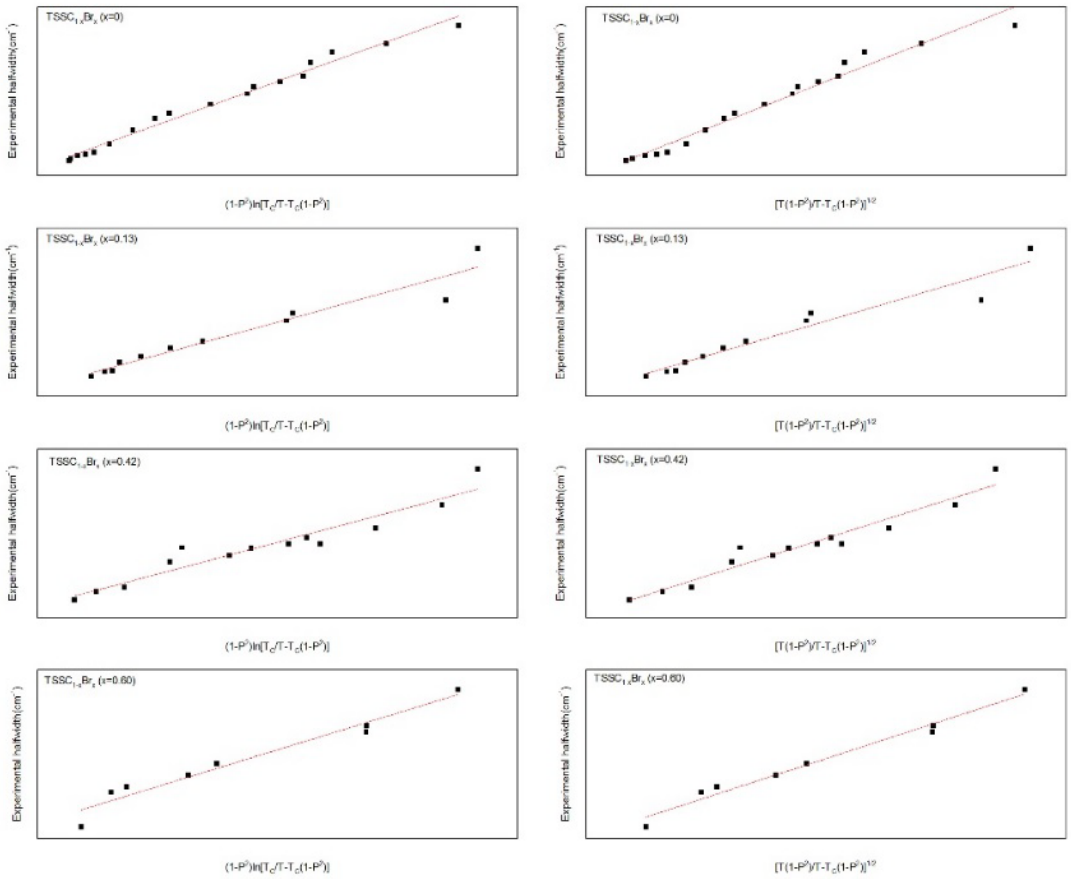

Figure 2 The experimental halfwidth [9] against our calculated Γ_{SP} Eqs. (1) - (2) of the soft Raman modes at various temperatures in the ferroelectric phases of $TSSC_{1-x}Br_x$ (x = 0, 0.13, 0.42 and 0.60). The solid lines represent the best fit to the experimental data according to Eqs. (1) - (2) with the coefficients Γ_0' (Γ_0) and A' (A).

The temperature dependence of the damping constant (halfwidth) for the soft Raman modes in pure (x = 0) and brominated (x = 0.13, 0.42 and 0.60) $TSSC_{1-x}Br_x$ was calculated from both PS Eq. (1) and EF Eq. (2) models. For this calculation we consider that the observed [9] wavenumber (ω) of the soft Raman modes studied here is proportional to the order parameter P Eq. (3) according to;

$$\omega/\omega_{max} \propto P \tag{4}$$

where ω_{max} is the maximum value of the observed [9] wavenumber for the soft Raman modes studied here (**Table 1**). The critical temperature T_C of these soft Raman modes was also given in **Table 1**. The temperature dependence of the order parameter P Eq. (3) and also the observed [9] wavenumber (ω/ω_{max}) were plotted in **Figure 1** below the phase transition temperature T_C of the soft Raman modes studied here. Then, the PS model Eq. (1) and EF model Eq. (2) were used to evaluate the halfwidth of the soft Raman modes in $TSSC_{1-x}Br_x$ from their observed [9] wavenumbers (ω/ω_{max}) under the light of our consideration Eq. (4), **Figure 1** below the phase transition temperature T_C (ferroelectric phase). A fitting procedure for the halfwidths was employed between the calculated values Eqs. (1) - (2) and the observed [9] data of the soft Raman modes studied in $TSSC_{1-x}Br_x$ (x = 0, 0.13, 0.42 and 0.60) as given in **Figure 2**. This fitting procedure (**Figure 2**) allows us to extract the background damping constant Γ_0' (Γ_0) and the constant A' (A) of Eqs. (1) - (2) from the intercept points and the slopes, respectively, as we tabulated them in **Table 2**. The calculated values of the halfwidth (damping constant) from both PS and EF models Eqs. (1) - (2) and the observed [9] data were given in **Figure 3** at various temperatures for the soft Raman modes in the ferroelectric phase of $TSSC_{1-x}Br_x$ crystals with x = 0, 0.13, 0.42 and 0.60.

Bartoli and Litovitz [42] derived an expression to calculate the activation energy U from the damping constant (halfwidth) reads as;

$$\Gamma \cong \Gamma_{vib} + C \exp(-U/k_B T) \quad (5)$$

where C is a constant and k_B is the Boltzmann constant. The first term of Eq. (5), Γ_{vib} which refers to the vibrational relaxation is comparably small in the vicinity of the phase transition temperature T_C and it can be neglected. So, the activation energy U can be calculated as;

$$\ln\Gamma \cong \ln C \ -(U/k_B T) \quad (6)$$

Table 3 Values of the activation energy U and the constant $\ln C$ Eq. (6) due to pseudospin-phonon coupled (PS) model Eq. (1) and the energy fluctuation (EF) model Eq. (2) for the ferroelectric-paraelectric transition in $TSSC_{1-x}Br_x$ (x = 0, 0.13, 0.42 and 0.60). $k_B T_C$ values are also given here.

Crystal	Models	U (meV)	$\ln C$	Temperature interval (K)	$k_B T_C$ (meV)
$TSSC_{1-x}Br_x$ (x = 0)	PS Eq. (1)	113	13	121.7 < T < 127.8	11
	EF Eq. (2)	133	15		
$TSSC_{1-x}Br_x$ (x = 0.13)	PS Eq. (1)	62	8	104.1 < T < 119.3	10
	EF Eq. (2)	67	9		
$TSSC_{1-x}Br_x$ (x = 0.42)	PS Eq. (1)	34	7	77.7 < T < 84.2	8
	EF Eq. (2)	38	8		
$TSSC_{1-x}Br_x$ (x = 0.60)	PS Eq. (1)	6	3	39.1 < T < 57.3	5
	EF Eq. (2)	6	3		

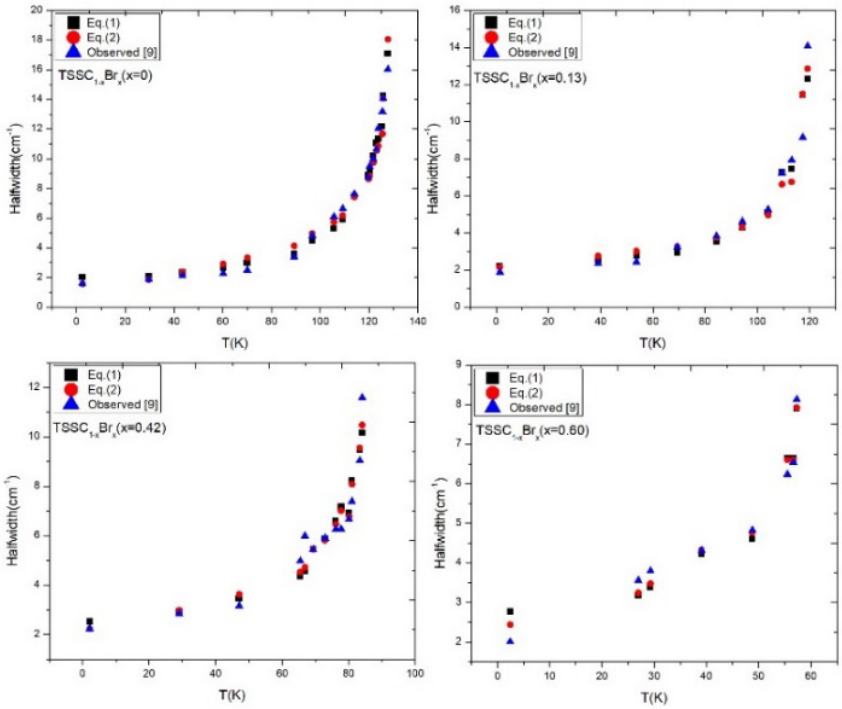

Figure 3 Damping constant (Γ_{SP}) calculated as a function of temperature using the pseudospin-phonon coupled (PS) and the energy fluctuation (EF) models according to Eqs. (1) - (2), respectively for soft Raman modes in the ferroelectric phases of $TSSC_{1-x}Br_x$ (x = 0, 0.13, 0.42 and 0.60). Observed [9] halfwidth data are also shown here.

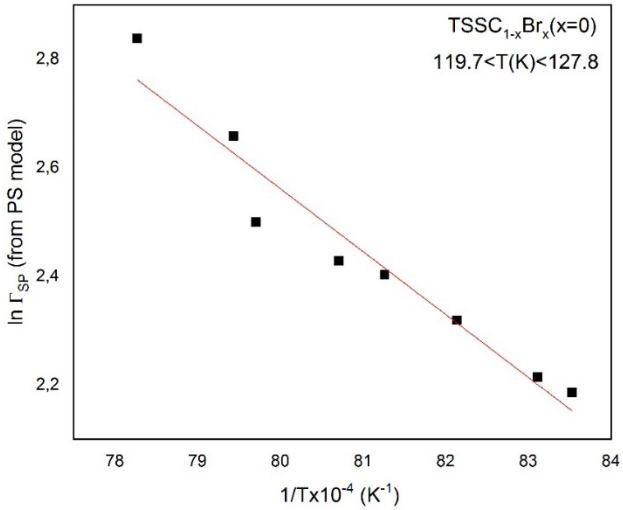

Figure 4 Temperature dependence of the damping constant calculated using the pseudospin-phonon coupled model Eq. (1) for the soft Raman mode to extract the value of the activation energy U according to Eq. (6) for the ferroelctric phase ($T < T_C$) of $TSSC_{1-x}Br_x$ ($x = 0$).

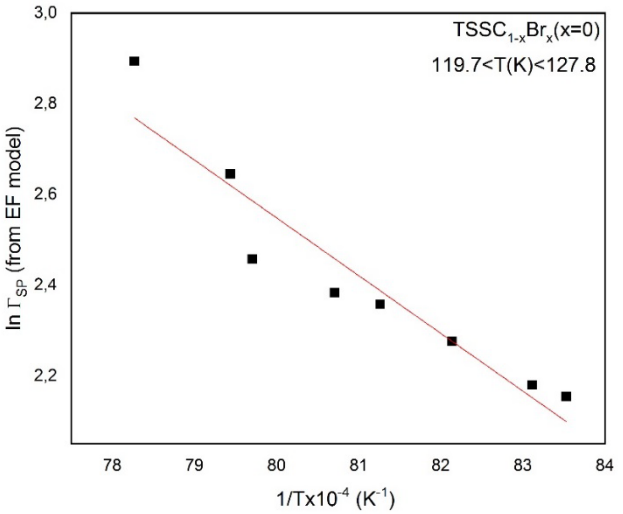

Figure 5 Temperature dependence of the damping constant calculated using the energy fluctuation model Eq. (2) for the soft Raman mode to extract the value of the activation energy U according to Eq. (6) for the ferroelctric phase ($T < T_C$) of $TSSC_{1-x}Br_x$ ($x = 0$).

The activation energy U and the constant $\ln C$ were extracted through Eq. (6) for the $TSSC_{1-x}Br_x$ ($x = 0$, 0.13, 0.42 and 0.60) by using the calculated values of the halfwidth (damping constant) from the PS Eq. (1) and EF Eq. (2) models (**Figures 4** and **5**). Those extracted values of the activation energy U and the constant $\ln C$ were given in **Table 3** in the temperature intervals considered.

Discussion

The 2 models (PS and EF) predict the temperature dependence of the damping constant (halfwidth). When the bandwidths of the Raman and IR spectra for the phonon modes are measured experimentally, they can be compared directly with the predicted damping constants. Also, the activation energy can be determined in a crystalline system experimentally. It can be compared with the activation energies predicted due to the various phonon modes by the present models (PS and EF). For both reasons, those models need to be considered in this study.

The temperature dependence of the wavenumber ω for the soft Raman modes in pure (x = 0) and brominated (x = 0.13, 0.42 and 0.60) TSSC, $TSSC_{1-x}Br_x$ **,** anomalously decreases with increasing temperature as T_C is approached from the ferroelectric phase ($T < T_C$) as observed experimentally [9]. This behavior is very similar to the order parameter P predicted from the mean field theory [41] as shown in **Figure 1**. Since the order parameter can take any value between 0 and 1, the normalized wavenumber ω with respect to its maximum value ω_{max} (ω/ω_{max}) was used as plotted in **Figure 1**. This good agreement between ω and P allows us to consider that the observed wavenumber ω/ω_{max} of the soft Raman modes in $TSSC_{1-x}Br_x$ studied here can be associated with the order parameter according to Eq. (4). Since the spontaneous polarization (P) was used as an order parameter for both models (PS and EF) to study the phase transitions in the KDP type crystals [28,29,40], the temperature dependence of the wavenumber (ω) was then considered to govern the mechanism of the order-disorder transition at T = 247 K in $TSSC1_{-x}Br_x$ (x = 0, 0.13, 0.42 and 0.60). Thus, in analogy with the ω, the temperature dependence of the spontaneous polarization was the preliminary parameter in our treatment given here. Using the observed wavenumbers [9] of the soft Raman modes as the variation of the order parameter P with the temperature in Eqs. (1) - (2), we predicted the halfwidth (damping constant) Γ_{SP} due to the pseudospin-phonon interactions in $TSSC_{1-x}Br_x$ (x = 0, 0.13, 0.42 and 0.60) for the ferroelectric phase. The predicted values of the halfwidth from both pseudospin-phonon coupled (PS) model Eq. (1) and the energy fluctuation (EF) model Eq.2) were then fitted to the observed [9] halfwidths of the soft Raman modes in $TSSC_{1-x}Br_x$ (**Figure 2**) with the fitted parameters as given in **Table 2**. The calculated Γ_{SP} values from both models Eqs. (1) - (2) are in good agreement with the observed halfwidths [9] of the soft Raman modes in $TSSC_{1-x}Br_x$ (x = 0, 0.13, 0.42 and 0.60) as shown in **Figure 3**. This figure gives the divergence behavior of the damping constant Γ_{SP} due to the pseudospin-phonon coupling as observed experimentally [9] for the halfwidth of the soft Raman modes in the ferroelectric phase as T_C is approached in $TSSC_{1-x}Br_x$ (x = 0, 0.13, 0.42 and 0.60). This is an indication of that both PS Eq. (1) and EF Eq. (2) models adequately describe the mechanism of the ferroelectric-paraelectric phase transition in $TSSC_{1-x}Br_x$ (x = 0, 0.13, 0.42 and 0.60) on the basis of the observed [9] wavenumbers (**Figure 1**) and the halfwidths of the soft Raman modes involving these transitions.

The values of the activation energy U as well as the constant $\ln C$ were then extracted (**Table 3**) according to Eq. (6) for the ferroelectric phases of $TSSC_{1-x}Br_x$ (x = 0, 0.13, 0.42 and 0.60). This extraction was performed from the halfwidth calculated in Eqs. (1) - (2) of the soft Raman modes within the temperature ranges studied (**Table 3**) due to the both pseudospin-phonon coupled (PS) model and the energy fluctuation (EF) model. A linear variation of $\ln\Gamma$ with $1/T$ according to Eq. (6) was plotted in **Figures 4** and **5**, respectively, in the ferroelectric phase of $TSSC_{1-x}Br_x$ (x = 0). As one can see easily from **Table 3**, the values of the activation energy deduced from both PS and EF models decrease as the bromine concentration x increases. In addition, our calculated values of the activation energy U from both models (PS and EF) for $TSSC_{1-x}Br_x$ are larger than the k_BT_C (up to the 10 times) of the compounds with x = 0, 0.13 and 0.42 which indicate that the transition between the ferroelectric and paraelectric phases is of an order-disorder type in these compounds as pointed out previously for $LiNH_4SO_4$ [42] on the basis of the activation energy. On the other hand, the extracted values of the activation energy from both PS and EF models for the $TSSC_{1-x}Br_x$ (x = 0.60) are closer to the k_BT_C value for this compound (**Table 3**). Note that, the k_BT_C value, that is independent of the models studied here, characterizes the activation energy at the transition temperature between the ferroelectric and paraelectrric phases in the $TSSC_{1-x}Br_x$. In particular, the activation energy value of 0.113 eV (10.9 kJ/mol) deduced from the PS model within the temperature interval of $121.7 < T(K) < 127.8$ of TSSC (x = 0) and also the value of 0.133 eV (12.8 kJ/mol) deduced from the EF model within the same temperature of TSSC (x = 0) can be compared with that reported value of 11.5 kJ/mol of the same compound [17]. We have found no reported values of the activation energy for the brominated TSSC in the literature to compare with.

Conclusions

Analysis of the critical behavior of some dynamic quantities such as the wavenumber, the halfwidth and the activation energy of $TSSC_{1-x}Br_x$ (x = 0, 0.13, 0.42 and 0.60) close to the phase transition temperatures on the basis of the theoretical models (EF and PS) may give some clues regarding the nature of the phase transition mechanism. Our calculated values of the halfwidths from both PS and EF models, by associating the wavenumbers of the soft Raman modes with the order parameter, fit well to the observed behavior. This is an indication of that the phase transition mechanism of $TSSC_{1-x}Br_x$ is mainly driven by the soft Raman modes in the compounds studied here. Furthermore, our calculated values of the activation energy (close to the phase transition temperatures) are much larger than the k_BT_C values, which

is a sign for the order-disorder type, phase transition mechanism in the compounds of $TSSC_{1-x}Br_x$. As a result, both PS and EF models are adequate to describe the phase transition mechanism of $TSSC_{1-x}Br_x$, and both of them can be used to explain the phase transition mechanism of some other ferroelectric liquid crystals.

References

[1] Y Makita. Ferroelectricity in $(CH_3NHCH_2COOH)_3 \cdot CaCl2$. *J. Phys. Soc. Jpn.* 1965; **20**, 2073-80.

[2] GE Feldkamp, JF Scott and W Windsch. Light scattering study of phase transitions in ferroelectric tris-sarcosine calcium chloride and its brominated isomorphs. *Ferroelectrics* 1981; **39**, 1163-6.

[3] SPP Jones, DM Evans, MA Carpenter, SAT Redfern, JF Scott, U Straube and VH Schimdt. Phase diagram and phase transitions in ferroelectric tris-sarcosine calcium chloride and its brominated isomorphs. *Phys. Rev. B* 2011; **83**, 094102.

[4] T Ashida, S Bando and M Kakudo. The crystal structure of trissarcosine calcium chloride. *Acta Crystallogr. B* 1972; **B28**, 1560-5.

[5] M Mishima, K Ito and E Nakamura. Structure of calcium chloride-sarcosine (1/3), $CaCl_2.3C_3H_7NO_2$, in the ferroelectric phase. *Acta Crystallogr. C* 1984; **40**, 1824-7.

[6] G Sorge and U Straube. Dielectric behaviour of ferroelastic monodomain TSCC crystals. *Phys. Status Solidi* 1979; **51**, 117-21.

[7] SD Prokhorova, GA Smolensky, IG Siny, EG Kuzminov, VD Mikvabia and H Arndt. Light scattering study of the phase transition in TSCC. *Ferroelectrics* 1980; **25**, 629-32.

[8] M Sugo, M Kasahara, M Tokunaga and I Tatsuzaki. Raman scattering study of the soft mode in ferroelectric $(CH_3NHCH_2COOH)_3CaCl_2$. *J. Phys. Soc. Jpn.* 1984; **55**, 3234-41.

[9] T Chen and G Schaack. Spectroscopic investigation of the ferroelectric phase transition in tris-sarcosine calcium chloride: An order-disorder system with displacive features. I. Experimental results. *J. Phys. C Solid State Phys.* 1984; **17**, 3801-20.

[10] LC Brunel, JC Bureau, S Wartewig and W Windsch. Raman scattering study of the ferroelectric phase transition in tris-sarcosine calcium chloride (tscc). *Chem. Phys. Lett.* 1980; **72**, 119-21.

[11] T Chen, G Schaack and V Winterfeldt. Raman and infrared spectroscopy of tris-sarcosine calcium chloride bromide ($TSCC_{1-x}B_x$, $0 \leq \times \leq 1$). *Ferroelectrics* 1981; **39**, 1131-4.

[12] E Nakamura, K Ito, K Deguchi and N Mishima. Mechanism of the ferroelectric phase transition in tris-sarcosine calcium chloride. *Jpn. J. Appl. Phys.* 1985; **24**, 393-5.

[13] W Windsch, H Braeter and J Riedl. Concentration and temperature dependences of the order parameter and the soft optic mode of the solid solution TSCC and TSCB. *Solid State Comm*. 1985; **53**, 621-5.

[14] GV Kozlov, AA Volkov, JF Scott, GE Feldkamp and J Petzelt. Millimeter-wavelength spectroscopy of the ferroelectric phase transition in tris-sarcosine calcium chloride (CH3NHCH2COOH)·3CaCl2. *Phys. Rev. B* 1983; **28**, 255-61.

[15] D Michel, U Hacker, T Erge and J Petersson. NMR investigations of molecular motions and critical dynamics at the ferroelectric phase transition of tris-sarcosine calcium chloride. *Phys. Status Solidi B* 1994; **185**, 257-64.

[16] M Fujimoto, S Jerzek and W Windsch. Order-disorder dynamics of the ferroelectric phase transition in tris-sarcosine calcium chloride crystals. *Phys. Rev. B* 1986; **34**, 1668-76.

[17] K Lee, M Lee, KS Lee and AR Lim. ^{1}H NMR study of the phase transitions of trissarcosine calcium chloride single crystals at low temperature. *J. Phys. Chem. Solid.* 2005; **66**, 1739-43.

[18] T Hikita, P Schnackenberg and VH Schmidt. Brillouin scattering study of the ferroelectric phase transition in tris-sarcosine calcium chloride. *Phys. Rev. B* 1985; **31**, 299-303.

[19] T Chen and G Schaack. Spectroscopic investigation of the ferroelectric phase transition in tris-sarcosine calcium chloride: An order-disorder system with displacive features. II. Soft modes in pseudo-spin-phonon coupled systems. *J. Phys. C Solid State Phys.* 1984; **17**, 3821.

[20] VH Schmidt. Cluster model for tris-sarcosine calcium chloride (TSCC) describing order-disorder and displacive features of its ferroelectric transition and its pressure-induced transition to an antiferroelectric phase. *Ferroelectrics* 1981; **39**, 1151-4.

[21] S Fujimoto and N Yasuda. Dielectric loss tangent of trissarcosine calcium chloride under hydrostatic pressure. *Jpn. J. Appl. Phys.* 1982; **21**, 1386.

[22] R Navalgund and LC Gupta. Electron paramagnetic resonance study of Mn^{2+} in ferroelectric lithium ammonium tartarate monohydrate. *Solid State Comm*. 1976; **19**, 1205-7.

[23] EV Treck and W Windsch. EPR investigations of solid solutions of TSCC and TSCB doped with Mn^{2+}. *Kristall und Tech.* 1978; **13**, 513-6.
[24] S Fujimoto, N Yasuda, H Kashiki, K Takagi and M Fujimoto. Dielectric properties of solid solutions of trissarcosine calcium chloride (TSCC) and bromide (TSCB). *Ferroelectrics* 1981; **39**, 1139-42.
[25] JC Lashley, JHD Munns, M Echizen, MN Ali, SE Rowley and JF Scott. Phase transition in brominated ferroelectric tris-sarcosine calcium chloride. *Adv. Mater.* 2014: **26**, 3860-6.
[26] R Blinc and B Zeks. Dynamics of order-disorder-type ferroelectrics and antiferroelectrics. *Adv. Phys.* 1972; **21**, 693-757.
[27] Y Tezuka and S Shin. Hyper-Raman and raman studies on the phase transition of ferroelectric $LiTaO_3$. *Phys. Rev. B* 1994; **49**, 9312-21.
[28] I Laulicht and N Luknar. Internal-mode line-broadening by proton jumps in KH_2PO_4. *Chem. Phys. Lett*. 1977; **47**, 237-40.
[29] I Laulicht. On the drastic temperature broadening of hard mode Raman lines of ferroelectric KDP type crystals near Tc. *J. Phys. Chem. Solids* 1978; **39**, 901-6.
[30] G Schaack and V Winterfeldt. Temperature behaviour of optical phonons near Tc in triglycine sulphate and triglycine selenate. *Ferroelectrics* 1977; **15**, 35-41.
[31] A Kiraci and H Yurtseven. Temperature dependence of the raman frequency, damping constant and the activation energy of a soft-optic mode in ferroelectric barium titanate. *Ferroelectrics* 2012; **432**, 14-21.
[32] H Yurtseven and A Kiraci. Calculation of the damping constant and the relaxation time for the soft-optic and acoustic mode in hexagonal barium titanate. *Ferroelectrics* 2012; **437**, 137-48.
[33] H Karacali, A Kiraci and H Yurtseven. Calculation of the Raman frequency and the damping constant of a coupled mode in the ferroelectric and paraelectric phases in KH_2PO_4. *Phys. Status Solidi B* 2010; **247**, 927-36.
[34] A Kiraci and H Yurtseven. Damping constant and the relaxation time calculated for the lowest-frequency soft mode in the ferroelectric phase of $Cd_2Nb_2O_7$. *Optik* 2016; **127**, 11497-504.
[35] A Kiraci and H Yurtseven. Calculation of the raman frequency, damping constant (Linewidth) and the relaxation time near the tetragonal-cubic transition in $PbTiO_3$. *Optik* 2017; **142**, 311-9.
[36] H Yurtseven and A Kiraci. Temperature dependence of the damping constant and the relaxation time close to the tetragonal-cubic phase transition in $SrZrO_3$. *J. Mol. Struct.* 2017; **1128**, 51-6.
[37] H Yurtseven and A Kiraci. Damping constant (linewidth) and the relaxation time of the brillouin la mode for the ferroelectric-paraelectric transition in $PbZr_{1-x}Ti_xO_3$. *IEEE Trans. Ultrason. Ferroelectrics Freq. Contr.* 2016; **63**, 1647-55.
[38] A Kiraci and H Yurtseven. Analysis of the integrated intensity of the central peaks calculated as a function of temperature in the ferroelectric phase of lithium tantalite. *Therm. Sci.* 2018; **22**, 221-7.
[39] H Yurtseven and A Kiraci. Damping constant and the inverse relaxation time calculated as a function of pressure using the x-ray diffraction data close to the cubic-tetragonal phase transition in $SrTiO_3$. *Ferroelectrics* 2019; **551**, 143-51.
[40] G Lahajnar, R Blinc and S Zumer. Proton spin-lattice relaxation by critical polarization fluctuations in KH_2PO_4. *J. Phys. Condens. Matter* 1974; **18**, 301-16.
[41] M Matsushita. Anomalous temperature dependence of the frequency and damping constant of phonons near T_λ in ammonium halides. *J. Chem. Phys.* 1976; **65**, 23-8.
[42] MA Hossain, JP Srivastava, PK Khulbe, L Menon and HD Bist. A Raman study of the high temperature phase transition in lithium ammonium sulphate. *J. Phys. Chem. Solids* 1994; **55**, 85-90.